Diamond & Related Materials 142 (2024) 110763

Contents lists available at ScienceDirect

Diamond & Related Materials

journal homepage: www.elsevier.com/locate/diamond

Synthesis and characterization of Restricted Access Magnetic Nanotubes (M-RACNTs) for the extraction of secondary metabolites from *Lasiodiplodia* sp. fermentation broth

Cristiane dos R. Feliciano [a], Heloisa Sales de Souza [a], Vinicius Câmara Costa [b], Omar Cabezas Gómez [c], Jaine Honorata Hortolan Luiz [c], Luiz Fernando Gorup [d,e,f,g], Mariane Gonçalves Santos [a,*]

[a] *Toxicants and Drugs Analysis Laboratory - LATF, Faculty of Pharmaceutical Sciences, Federal University of Alfenas - Unifal-MG, Alfenas, MG 37130-000, Brazil.*
[b] *Embrapa Instrumentation, São Carlos, SP 13560-970, Brazil.*
[c] *Bioprocess Laboratory - BIOPRO, Chemistry Institute, Federal University of Alfenas - Unifal-MG, Alfenas, MG 37130-000, Brazil*
[d] *Institute of Chemistry, Federal University of Alfenas, 37130-001 Alfenas, MG, Brazil*
[e] *LIEC - Department of Chemistry, Federal University of São Carlos, Rod. Washington Luis km 235, CP 676, São Carlos, SP 13565-905, Brazil*
[f] *School of Chemistry and Food Science, Federal University of Rio Grande, Av. Italia km 8 Bairro Carreiros, Zip Code: 96203-900 Rio Grande, RS, Brazil*
[g] *Materials Engineering, Federal University of Pelotas, Campus Porto, 96010-610 Pelotas, RS, Brazil*

ARTICLE INFO

Keywords:
Restricted access materials
Nanocomposite
Endophytic fungi
Lasiodiplodia sp.
Dispersive solid-phase extraction
Magnetic carbon nanotubes

ABSTRACT

This work proposed the synthesis and the characterization of Restricted Access Magnetic Nanotubes (M-RACNTs) to be used as sorbent in the magnetic dispersive solid-phase extraction (MDSPE) of organic compounds from the fermentation broth of the endophyte *Lasiodiplodia* sp. Synthesis was performed by functionalizing commercial multiple-walled carbon nanotubes with magnetic nanoparticles (M-CNTs) and by coating the M-CNTs with a layer of bovine serum albumin. The materials were characterized by infrared spectroscopy with Fourier Transform, thermogravimetry, zeta potential, and scanning electron microscopy. Different crude extracts were obtained, depending on the sample pH and the elution solvent tested. Chloroform and ethyl acetate extracts showed activity against a Gram-positive pathogen (*Staphylococcus aureus*). The crude extract's constitution was investigated. By GC/MS analysis were found hydrocarbons, aldehydes, alcohols, among others, while by LC-MS/MS analysis were found flavonoids, macrocyclic lactones, oleic acids, jasmonic acid derivatives and amino acids. A multivariate optimization, through fractional factorial planning, for four independent variables, was performed for a hydrocarbon (hexadecane) and one possible jasmonic acid derivative, both with antimicrobial activity related in the literature. The results showed that it was possible to obtain crude extracts with high concentrations of these analytes in a single extraction procedure. The increase in the analytical signal was 3.7 times for hexadecane and 1.4 times for the possible jasmonic acid derivative. The M-RACNTs also demonstrated their ability to prevent the adsorption of macromolecules, such as lysozyme, which was confirmed through SDS-PAGE analysis.

1. Introduction

The fermentation broths of endophytic fungi have been considered an important source of bioactive secondary metabolites useful for the pharmaceutical and food industries. Many studies have shown that these metabolites present a wide variety of biological activities, such as fungicidal [1], bactericidal [1], and antitumor [2] activity. In addition to low molecular weight compounds, the fermentation broth contains macromolecules, such as peptides, proteins, and polysaccharides. Thus, due to their great potential as a source of bioactive substances, the fermentation broths of endophytic fungi have been extensively investigated to identify and isolate new secondary metabolites or obtain those with known activity in great amounts. One of the major problems faced by this type of research is that traditional techniques used in the sample preparation process cannot provide crude extracts with sufficient quantities of interesting compounds to undergo new separation and

* Corresponding author.
E-mail address: mariane.goncalves@unifal-mg.edu.br (M.G. Santos).

https://doi.org/10.1016/j.diamond.2023.110763
Received 2 September 2023; Received in revised form 4 December 2023; Accepted 25 December 2023
Available online 2 January 2024

purification procedures.

Currently, the main sample preparation technique utilized to obtain bioactive substances from the fermentation broth is liquid-liquid extraction (LLE). In this case, organic solvents of different polarities are used to extract organic compounds based on their solubility in the organic and aqueous phase. However, LLE presents some drawbacks, such as low selectivity, low recovery, the fact that large volumes of sample and solvent are required, and the possibility of emulsion formation, which can cause sample losses and contamination [3]. On this basis, the development of new sorbents and methods that can retain and pre-concentrate bioactive products from the fermentation broth of endophytic fungi is promising and indispensable. Regarding this scenario, some sample preparation strategies were successfully used for this purpose, such as solid-phase microextraction (SPME) [4] and traditional solid-phase extraction (SPE) based on porous ion exchange resin [5].

The dispersive solid-phase extraction (D-SPE) technique is based on the dispersion of a solid sorbent in a liquid sample, for the extraction and clean-up process. The dispersion process increases the contact area between the sorbent and the analyte and enables a good interaction between the sample and the sorbent. D-SPE has been widely applied as a technique of extraction, isolation, and cleaning of various organic compounds from complex samples in analytical processes. Its advantages lie in its simplicity, robustness, selectivity, and minimized solvent consumption [6,7]. When a magnetic sorbent is used, this procedure is still simplified because an external magnet can be used to separate the sorbent from the sample [6], removing the centrifugation and filtration steps. Magnetic sorbents can be obtained through the introduction of magnetic nanoparticles (MNPs) in the pores of traditional sorbents, e.g., polymers [8,9], graphene [10], metal-organic structures [11,12], and carbon nanotubes (CNTs) [13], among others. M-CNTs (Magnetic Carbon Nanotubes) have been related as being excellent sorbents for MDSPE due to their high surface area and high chemical as well as physical stability [14].

Still referring to sample preparation techniques, the presence of macromolecules, such as proteins, in biological samples can significantly interfere with the efficiency of the extraction procedure, reducing the recovery and selectivity, because they can be adsorbed and block the analyte binding site. In addition, macromolecules are incompatible with most analytic techniques, including chromatography [15]. To solve this problem, intelligent materials capable of excluding proteins, for example, and retaining analytes of low molecular weight have been used in sample preparation methods. RAMs (Restricted Access Materials) are a class of sorbent capable of performing this task. These materials usually present a hydrophilic external layer capable of preventing the adsorption of macromolecules by physical and chemical mechanisms and retaining only the interesting molecules in their pores [15]. RAMs can be obtained by modifying silica [16], organic polymers [17], carbon nanotubes [18], and graphene [19].

So, in this study, we synthesized a composite that combines the good adsorption capacity and versatility of M-CNTs with the capacity to avoid macromolecule adsorption of RAMs, resulting in the generation of M-RACNTs (Magnetic Bovine Serum Albumin-Covered Restricted Access Carbon Nanotubes) to be used as a sorbent in the MDSPE of secondary metabolites from the fermentation broth of *Lasiodiplodia* sp., a new application for this kind of sorbent, not yet related in the literature.

2. Material and methods

2.1. Reagents and solutions

Multi-walled carbon nanotubes (MWCNTs) (purity 95 %), with external diameters from 6 to 9 nm and lengths of 5 μm, iron (II) chloride ($FeCl_2{\cdot}4H_2O$), BSA, and sodium borohydride ($NaBH_4$) were obtained from Sigma-Aldrich (Steinheim, Germany). Iron (III) chloride hexahydrate ($FeCl_3{\cdot}6H_2O$) was acquired from Vetec® (Rio de Janeiro, Brazil). Ammonium hydroxide (NH_4OH) and isopropyl alcohol were obtained from Isofar® (Rio de Janeiro, Brazil). Hydrochloric acid (HCl) was purchased from Exodus Scientifica (São Paulo, Brazil). Glutaraldehyde was obtained from Rioquímica (São José do Rio Preto, Brazil). Monobasic and dibasic potassium phosphates, sodium hydroxide (NaOH), and sodium chloride (NaCl) were acquired from Synth (Diadema, Brazil). Formic acid was obtained from Vetec®. Organic solvents (chromatographic grades) such as ethyl acetate and chloroform, were obtained from ACS (Sumaré, São Paulo), and hexane and acetonitrile were obtained from Dinâmica (Indaiatuba, São Paulo). Ultrapure water (18.2 MΩcm) was obtained from a Milli-Q water purification system (Millipore, Bedford, USA). For the fermentation process, glucose was obtained from ALPHATEC (São Paulo, São Paulo), sodium nitrate ($NaNO_3$) and potassium phosphate were obtained from Dinâmica, potassium chloride was obtained from ACS, iron sulfate was obtained from Lafan (Várzea Paulista, São Paulo), yeast extract was obtained from Isofar (Duque de Caxias, Rio de Janeiro), and magnesium sulfate heptahydrate was purchased from Vetec®. For the biological test, Mueller Hinton and Sabouraud medium were obtained from HIMEDIA (Mumbai, India) and RPMI-1649 was obtained from Sigma-Aldrich.

2.2. Synthesis of M-RACNTs

The M-RACNTs were obtained in two steps according to the procedure below:

(i) First step: The M-CNTs were prepared by the co-precipitation method according to Qu et al., (2007) [20], with some modifications. For that, 0.423 g of $FeCl_3.6H_2O$ and 0.625 g of $FeCl_2.4H_2O$ were solubilized in 300 mL of deionized water. This solution was heated at 50 °C and kept under nitrogen gas flow and vigorous stirring (300 rpm) for 5 min. Sequentially, 250 mg of multi-walled carbon nanotubes (MWCNTs) was added to the reactional media, and the suspension was stirred for 10 min. Then, 2.5 mL of 28–30 % NH_4OH (*w*/w) was added dropwise and stirring was maintained for >30 min. The total time of synthesis was 45 min. The M-CNTs were collected using an external magnet and were repeatedly washed with deionized water until neutral pH. The particles were dried under a vacuum atmosphere at 60 °C for 24 h.

(ii) Second step: To obtain the M-RACNTs, the M-CNTs were coated with BSA according to Barbosa et al.'s protocol [21]. For that, 500 mg of M-CNTs was placed into 5 mL polypropylene cartridges. Then, 20 mL of 1 % (*w/v*) BSA solution (prepared in 0.05 mol L^{-1} phosphate buffer pH 6.0) was percolated through the material. Afterward, 25 mL of 5 % (w/v) aqueous glutaraldehyde solution was placed in contact with the M-CNTs for 5 h to promote the crossover of the BSA molecules. Finally, 10 mL of $NaBH_4$1% (w/v) aqueous solution was percolated through the cartridges to stabilize the protein network. The M-RACNTs were washed with deionized water to remove reagent residues and were dried at 60 °C for 24 h.

2.3. Characterization studies

The infrared analyses were carried out on a Fourier transform infrared spectrometer (FT-IR) (model 8400S, Shimadzu®, Tokyo, Japan), with a spectral resolution of 4 cm^{-1}. The spectra monitored the range from 4000 to 400 cm^{-1} (32 scans).

Thermogravimetric analyses (TGA) were performed in a thermogravimetric analyzer, TG-DTA-SDT, Q600 model (TA Instruments, Castle, USA), operating from 25 to 800 °C, at a heating rate of 10 °C min^{-1}, under a nitrogen flow of 100 mL min^{-1}.

The zeta potentials were obtained using a Zetasizer Nano ZS equipped with an MPT-2 Titrator (Malvern, Worcestershire, UK). Aqueous suspensions (10 mL) of 5 mg mL^{-1} of CNTs, M-CNTs, and M-RACNTs were prepared individually. The suspensions were kept in an ultrasonic

bath for 30 min before analysis to improve dispersion. Then, 0.2 mL of each suspension was dispersed in 10 mL of 0.020 mol L^{-1} phosphate buffer solution at different pHs, ranging from 3.0 to 10.0.

The size and morphology of CNTs, M-CNTs, and M-RACNTs were analyzed by Scanning Electron Microscopy (SEM). A Zeiss Supra 35VP field effect electron gun (FEG-SEM) microscope was used, working at 5 to 15 keV and spot 3. To prepare the samples, small fragments of samples were added to a silicon substrate fixed with carbon tape. Lastly, the samples were oven-dried at 40 °C for 12 h. Scanning electron microscopy (SEM) is a high-resolution analysis technique commonly used to investigate the structure and morphology of materials at the micro and nanometric scales. SEM-EDS is particularly useful to investigate the interaction between nanoparticles and the surface of nanotubes, specifically the distribution of magnetite nanoparticles. Analyses of 2D energy dispersive x-ray detector, EDX, or EDS were performed with 2D mapping working at 25 keV and spot 4. This accessory device was essential in the characterization study of the dispersion of carbon, iron, and oxygen in the sample. When the electron beam strikes the material, the electrons in the inner layers of atoms are removed. The atoms of the levels just above occupy the position of the removed electron, in this process, the electron releases the quantized energy referring to the difference between the energy levels of the layer. A detector installed in the SEM vacuum chamber measured the energy associated with the emission of this electron. Since the electrons of a given atom have distinct energies, it was possible at the point of incidence of the beam to determine which chemical elements were present at that location and to identify the chemical composition in the observed area. Images 2D EDS were made by the energy released from the emission C Kα, O Kα, and Fe Lα1.

2.4. Fermentation process of Lasiodiplodia sp.

The endophytic fungi used in the study were isolated and classified in previous works. The isolation was carried out from healthy leaves of *Handroanthus impetiginosus*. The classification was performed by sequential DNA analysis and phylogenetic inference, resulting in the identification of *Lasiodiplodia* sp. [1].

The fungal isolate was subcultured on potato dextrose agar and incubated for 7 days in a Styrofoam box at room temperature (25 °C). After growth, the mycelium was picked and inoculated into Erlenmeyer flasks containing 150 mL of Czapek broth-fermentation medium (glucose 30.0 g, $NaNO_3$ 2.0 g, K_2HPO_4 1.0 g, $MgSO_4{\cdot}7H_2O$ 0.5 g, KCl 0.5 g, $FeSO_4{\cdot}7H_2O$ 0.01 g, yeast extract 1.0 g, diluted to 1000 mL of distilled water). The cultures were incubated at room temperature (25 °C) for 21 days. After the fermentation period, the culture medium was vacuum-filtered to remove the mycelium.

2.5. MDSPE procedure

Initially, the adsorptive capacity of M-RACNTs and the feasibility of their application in MDSPE were evaluated. The influence of pH in the extraction of substances belonging to different chemical classes was also evaluated here. As is known, many secondary metabolites are weak acids or bases and the pH can influence their degree of ionization, which affects the efficiency and selectivity of the extraction process. So, 150 mg of M-RACNTs were placed in 50.0 mL Falcon tubes containing 10.0 mL of the *Lasiodiplodia* sp. fermentation broth; its pH was adjusted to 3.0, 7.0, or 9.0 using HCl 3.0 mol L^{-1} or NaOH 3.0 mol L^{-1} solutions. The tubes were kept in an ultrasonic bath for 5 min. Then, the tubes were shaken for 45 min and the M-RACNTs particles were separated with a neodymium magnet. For the elution, 3.0 mL of organic solvent (chloroform, ethyl acetate, acetonitrile, or hexane) was added to the tubes containing the adsorbent. The tubes were shaken for 30 min and the M-RACNTs were separated with a magnet. The obtained extracts were dried and resuspended in 500 μL of the same organic solvent as that used in the elution process and were analyzed by GC–MS and LC-MS/MS. They were also evaluated for bactericidal, bacteriostatic, and antifungal activities.

After this step, two different compounds, one volatile and one polar (possibly hexadecane and a jasmonic acid derivative) were chosen as target analytes for performing the method optimization. For both, antimicrobial activity is reported in the literature [22,23]. The optimized MDSPE process for both hexadecane and the jasmonic acid derivative consisted of adding 150 mg of M-RACNTs to 50.0 mL Falcon tubes containing 10.0 mL of the *Lasiodiplodia* sp. fermentation broth at pH 7.0, sonicating the tubes for 5 min, shaking the tubes for 30 min, separating the M-RACNTs with a neodymium magnet, adding 3.0 mL of chloroform to the tubes, shaking for 10 min, and collecting the elution solvent. The extract was dried, resuspended in 500 μL of chloroform, and analyzed by GC–MS and LC-MS/MS. Only chloroform was selected as the elution solvent at this step because it was the one that presented the best antimicrobial activity.

2.6. Minimum inhibitory concentration (MIC) and minimum microbicide concentration (MMC) of crude extracts

The antimicrobial activity of crude extracts at pH 7.0, obtained with the elution solvents chloroform, ethyl acetate, acetonitrile, and hexane before the optimization process, has been determined by CLSI (Clinical and Laboratory Standards Institute) [19] methods, for yeast and bacteria, with some modifications. The test was performed in a Muller Hinton medium to assess activity against *Staphylococcus aureus* (ATCC 6538) and *Escherichia coli* (ATCC 25922), and in RPMI-1640 medium (Roswell Park Memorial Institute) to assess the activity against *Candida albicans* (ATCC 10231).

A mass of 200.0 mg of dried ethyl acetate and hexane extracts, separately, was solubilized in 25.0 mL of ethanol, and 200 mg of dried chloroform and acetonitrile extracts, were solubilized in 25 mL of dimethylsulfoxide, reaching the final concentration of 8.00 mg mL^{-1}. The solutions were placed in 96-well microplates under serial dilutions, from 400.00 to 3.125 μg mL^{-1}. The inoculum was prepared as a suspension and was standardized in a spectrophotometer at 660 nm (75 % transmittance), corresponding to 1.5×10^8 CFU·mL^{-1} (colony forming units per mL). Amoxicillin and streptomycin (10.00–0.078 μg mL^{-1}) for bacteria (Gram-positive and Gram-negative, respectively) and fluconazole (80–0.625 μg mL^{-1}) for yeast were used as positive controls. Culture media containing only the pathogens were used as negative controls. The microplates were incubated at 37 °C for 24 h. A 0.2 % aqueous resazurin solution was used as a revealing solution to determine inoculum viability through a change in color from blue to pink [1]. The MIC value was determined to be the lowest concentration, with no variation in the revealed color. All the extracts were studied in triplicate.

Considering that only the ethyl acetate and chloroform extracts showed antimicrobial activity against Gram-positive pathogens, only they were evaluated for the determination of MMC. For that, a 25 μL aliquot from these extracts was removed from the microplates that showed no color change (for samples and antimicrobials) and placed onto the surface of a Petri dish containing Muller Hinton agar (HIMEDIA, India). Each Petri dish was incubated at 37 °C for 24 h. The presence of bacteria on the plaque indicates that the extract presents bacteriostatic action. Otherwise, the absence of growth is indicative of bactericidal action.

2.7. Chromatographic analyses

The electron ionization (70 eV) mass spectrometric analysis was performed using a GC–MS QP-2010 from the Shimadzu® Corporation (Kyoto, Japan) equipped with an OPTIMA 5-MS (30 m × 0.25 mm × 0.25 μm) column, produced by Macherey-Nagel (Hœrdt, France) and a triple quadrupole analyzer. Pure helium (99.999 %) at a flow of 1.19 mL min^{-1} was used as the carrier gas. The samples were injected in the splitless mode (1 μL) and analyzed under the following conditions. The

initial temperature of the column was maintained at 80 °C for 2 min; this was raised to 200 °C at 12 °C min^{-1} and maintained at 200 °C for 5 min. The column temperature was then raised to 280 °C at 8 °C min^{-1} and remained constant for 4 min. The injector, interface, and ion source temperatures were 250, 250, and 200 °C, respectively. The analysis was achieved in SCAN mode, with an event time of 0.2 s, monitoring *m/z* ranging from 40.0 to 600.0. The obtained data were analyzed and compared to the Nist and MassBank databases.

LC-MS/MS analyses were performed using LC-MS 8030 equipment from Shimadzu® (Kyoto, Japan), equipped with a LiChrospher® 60 RP-select B (250.0 × 3.0 mm, 5.0 μm) chromatographic column (Darmstadt, Germany) and a triple-quadrupole mass analyzer. The oven, interface, and heat block temperatures were set to 40.0, 250.0, and 400.0 °C, respectively. The nebulizing and drying gas flow rates were 1.5 and 15.0 mL min^{-1}, respectively. The mobile phase of the chromatographic column was composed of 0.01 % formic acid aqueous solution–methanol at different proportions (*v*/v). The flow rate was 0.4 mL min^{-1}. Initially, until 5 min of the run, a proportion of 80:20 (v/v) formic acid aqueous solution–methanol was used; then the methanol proportion was increased to 30 % in 5 min and to 50 % in 10.00 min. This concentration was kept constant for 10 min, then increased to 100 % MeOH in 15 min. It remained constant for 5 min. Finally, the system returned to the initial condition with 20 % MeOH in 5 min, remaining constant for 15 min. The volume of the sample loop was 20.0 μL.

First, to select the precursor ions, the analyses were performed in SCAN mode (*m/z* ranging from 50.0 to 600.0), obtaining positive and negative electrospray ionization, simultaneously. Then, the analyses were carried out in Product Ion Scan mode. Each precursor was fragmented with 30ev collision energy, and a scan of the generated fragments was performed to obtain the mass fragmentation profile. The data files were acquired using the LabSolutions® software program, and the obtained spectra were processed on the GNPS platform (global natural products social molecular networking). The mass spectra data were first processed with the MZMINE2 [24,25] software and the results were then exported to GNPS. Molecular networks were obtained according to the following parameters: Data were filtered by removing all MS/MS fragment ions within ±17 Da of the precursor *m/z* and were window-filtered by choosing only the top 6 fragment ions in ±50 Da. The precursor ion mass tolerance was set to 0.05 Da and the MS/MS fragment ion tolerance to 0.05 Da. A molecular network was then created where edges were filtered to achieve a cosine score above 0.70 and >6 matched peaks. Further, edges between two nodes were kept in the network if and only if each of the nodes appeared in each other [26,27]. The GNPS data were then imported and visualized using the Cystoscope software (version 3.7.1) to improve the visibility and generate large as well as subnetwork portions.

2.8. Optimization of the extraction method by fractional factorial design

To demonstrate the possibility of improving recovery levels of target analytes by MDSPE method optimization, two distinct compounds that were identified in the chloroform extract and whose bactericidal activity is reported in the literature were selected as interesting analytes: one hydrocarbon (probably hexadecane, analyzed by GC–MS) and one possible jasmonic acid derivative (precursor *m/z* 213, analyzed by LC-MS/MS). Optimization was performed using a 2^{4-1} fractional factorial design, and the following independent factors were selected for the study: sorbent mass, adsorption time, elution solvent volume, and desorption time. As a response to the fractional factorial design, the area signal obtained for each analyte was used. A total of 11 experiments were performed including triplicate at the central point, which was used to estimate the experimental error. All factorial design experiments were performed at pH 7.00. The data obtained were processed using the StatSoft STATISTICA 10.0 software package (Tulsa, USA).

2.9. SDS-PAGE analysis

The analysis by SDS-PAGE was performed to investigate the protein constitution of the fermentation broth and the exclusion capacity of M-RACNTs. The fermentation broths were analyzed separately after extraction with M-RACNTs, at different pHs (ranging from 3.00 to 8.00 and without adjustment). First, the fermentation broth samples left over from the extraction process were dried in a vacuum oven for 18 h. Then they were dissolved in a buffer solution, in the proportion of 50 μL of sample to 150 μL of the buffer. SDS-PAGE analyses were performed in the Mini-Protean II Dual-Slab Cell (BioRad, USA), according to the methodology previously described by Laemmli [28]. The analysis was performed using 12 % polyacrylamide for the stacking and resolving gels, respectively. Low-range molecular mass standards (ranging from 14.4 to 97.4 kDa) from BioRad were used. The gels were stained with Coomassie Brilliant Blue R-250.

3. Results and discussion

3.1. Characterization

The FT-IR was performed for CNTs, M-CNTs, and M-RACNTs (Fig. 1). According to the spectra, all the materials presented a band from 2.960 to 2.850 cm^{-1}, which is characteristic of the stretching vibration of the C—H bond, and a band around 1.000–720 cm^{-1} related to C—C stretching vibration.

M-CNTs and M-RACNTs exhibited bands at about 550 cm^{-1}, corresponding to the stretching vibration of Fe—O, which suggests the presence of magnetite. M-RACNTs' spectra also presented a band at approximately 1450 cm^{-1}, related to Amide II, which indicates that the material was effectively covered by BSA [29] (Fig. 1).

The thermogravimetric curves are shown in Fig. 2. Weight loss for all the materials at temperatures lower than 200 °C can be attributed to water evaporation. CNTs presented 12 % of total weight loss; for M-CNTs, the total weight loss was about 6 %. This difference indicates that magnetite nanoparticles were incorporated into the CNTs' structure.

Fe_3O_4 is an inorganic material, so its degradation under an N_2 atmosphere (inert chemical environment) is unlikely. Thus, compared to CNTs, it was expected that M-CNTs would show a lower total weight loss value. M-RACNTs showed a total weight loss of 14 %. Compared to CNTs and M-CNTs, this increment can be related to the BSA network degradation and suggests that the coating process was satisfactory.

The variation of zeta potential as a function of pH was also evaluated. The isoelectric (Ip) points were 3.5, 4.0, and 4.8 for CNTs, M-CNTs, and M-RACNTs, respectively. The changes in Ip values indicate the incorporation of Fe_3O_4 nanoparticles in the CNTs' structure and the presence of the BSA layer on M-RACNTs (the Ip of pure BSA ranges from 4.7 to 4.9), according to the literature [30].

The zeta potential curves for CNTs, M-CNTs, and M-RACNTs are shown in Fig. 3. As can be observed, all the materials presented positive charges for pHs lower than Ip and negative charges for pHs higher than Ip (Fig. 3).

The magnetic susceptibility of M-RACNTs is demonstrated in Fig. 4. As it can be seen, even with a layer of BSA, in about 5 s, most M-RACNTs particles were attracted to the external neodymium magnet positioned in the test tube sidewall.

The size and morphology of the materials were analyzed through SEM (Fig. 5 a–d and Supplementary Material Figs. S1–S3) The images revealed that spherical Fe_3O_4 nanoparticles exhibited uniform morphology. The histogram of the SEM image of carbon nanotubes (Supplementary Material Fig. S3) demonstrates the mean diameter of 109.7 nm (Supplementary Fig. S4).

The SEM images (Fig. 5-b and c) showed the homogeneous distribution of magnetite nanoparticles in carbon nanotubes in the M-CNTs and M-RACNTs nanocomposites. The presence of magnetite nanoparticles on the surface of CNTs, along with their distribution in different

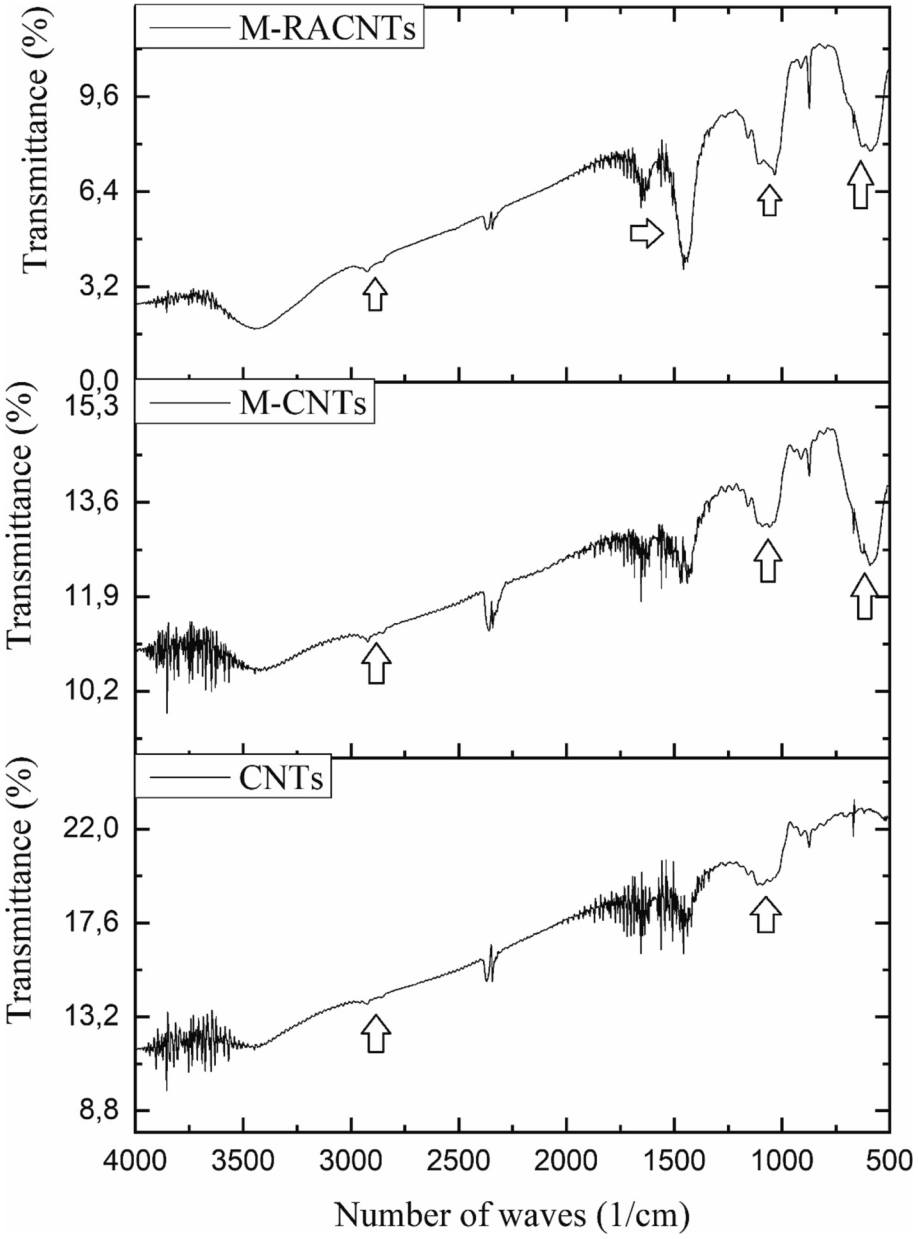

Fig. 1. FT-IR analysis of CNTs, M-CNTs, and M-RACNTs.

areas of the nanotubes, was observed. The homogeneous distribution of magnetite nanoparticles suggested that the particles were properly dispersed in the material, with no excessive concentration in specific areas of the CNTs. This finding is consistent with previous studies on carbon and magnetite nanotubes [20,31,32].

The dispersion of magnetite nanoparticles in carbon nanotubes can be evaluated using scanning electron microscopy techniques with secondary electrons (SE) and backscattered electrons (BSE), which are used to generate sample images that allow for the analysis of their spatial distribution [33,34]. Fig. 6a–d presents the secondary electron SEM images and the corresponding back-scattered SEM images of the as-prepared M-CNTs, and M-RACNTs nanocomposite.

The SEM-SE image (Fig. 6-a and c) showed that SE is sensitive to surface topography and composition, while BSE is sensitive to sample density and composition (Fig. 6-b and d) and is often used to analyze the distribution of heavy elements, such as iron, present in magnetite nanoparticles (white spots) dispersed in carbon nanotubes (translucent image).

In Fe_3O_4 nanoparticles, due to the virtue of their higher atomic number, backscatter more electrons than the low atomic weight carbon matrix and therefore generate brighter images. As shown in Fig. 6b–c, the bright Fe_3O_4 nanoparticle spots are well dispersed and embedded in the carbon matrix. Thus, the combination of SEM-SE and SEM-BSE provides detailed information on the dispersion of magnetite nanoparticles in M-CNTs, and M-RACNTs, allowing for the evaluation of their spatial distribution. The EDS analysis was performed to confirm the qualitative observations.

The homogeneous distribution of magnetite nanoparticles in carbon nanotubes can be influenced by several factors, such as the synthesis method, nanoparticle concentration, and reaction time. Li et al. [35], who employed the same EDS analysis methodology, reported similar results regarding magnetite particle homogeneous distribution in carbon nanotubes [35,36]. Some methodologies may lead to a non-homogeneous distribution of magnetite in carbon nanotubes [37,38].

SEM-EDS can also be used to analyze the chemical composition of the carbon nanotube system with magnetite nanoparticles [39,40]. Energy

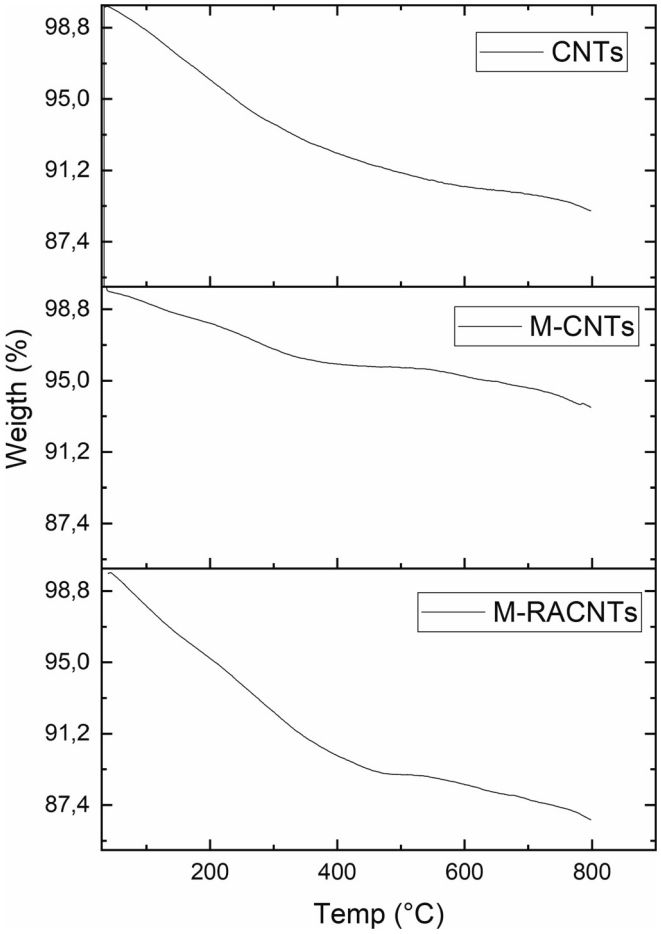

Fig. 2. Thermogravimetric analysis of CNTs, M-CNTs, and M-RACNTs.

Dispersive X-ray spectroscopy (EDS) can identify the presence of specific chemical elements, such as carbon, iron, and oxygen, and provide information about their distribution in the material [41].

SEM-EDS images show the magnetite and CNTs as a mixture and dispersed form M-CNTs (Supplementary Material Fig. S5), and M-RACNTs (Fig. 5-e–f and Supplementary Material Fig. S6) nanocomposites. The Energy Dispersive Spectroscopy (EDS) of the composites shows the presence of iron (Fe) and oxygen (O) of magnetite nanoparticles (yellow spots), and carbon (C) of carbon nanotube (magenta shades).

The 2D images were constructed by analyzing the energy released from the Fe Kα and O Kα (constituents of the magnetite material) (Fig. 5-f), and C Kα carbon nanotube (Fig. 5-e) emissions, indicating the uniform distribution of these elements in the demarcated area in the micrography of M-RACNTs. More information can be obtained by consulting Supplementary Material (Figs. S5 and S6).

Cui and Wang obtained similar results using the same synthesis methodology [37]. The SEM images cannot distinguish particle size because the particles are too close, but by the EDS (Supplementary Material Fig. S7) and XRD pattern (Supplementary Material Fig. S8) analyses are it possible to confirm the presence of iron oxide in the carbon nanotube composite.

The XRD pattern also confirms the presence of Fe_3O_4 nanoparticles. Fig. S8 in the Supplementary Material shows the X-ray diffraction patterns of conventional crystalline magnetite structures for M-CNTs and M-RACNTs nanocomposites.

As can be seen, all of the XRD patterns presented strong diffraction peaks in the ranges of $2\theta = 18.55°$, $30.81°$, $36.48°$, $43.52°$, $54.59°$, $56.83°$ and $62.34°$, corresponding to crystal planes (111), (220), (311), (222), (400), (422) and (511), respectively, matching well with the standard pattern of Fe_3O_4 nanoparticles. It is clear from these diffraction patterns that the prepared materials show all the characteristic reflections typical of face-centered cubic (fcc) crystal symmetry (PDF No. 86-1344) [42,43].

The mean crystallite diameter obtained from the diffractogram by using Scherrer's formula is 14,4 nm, which confirms the size observed

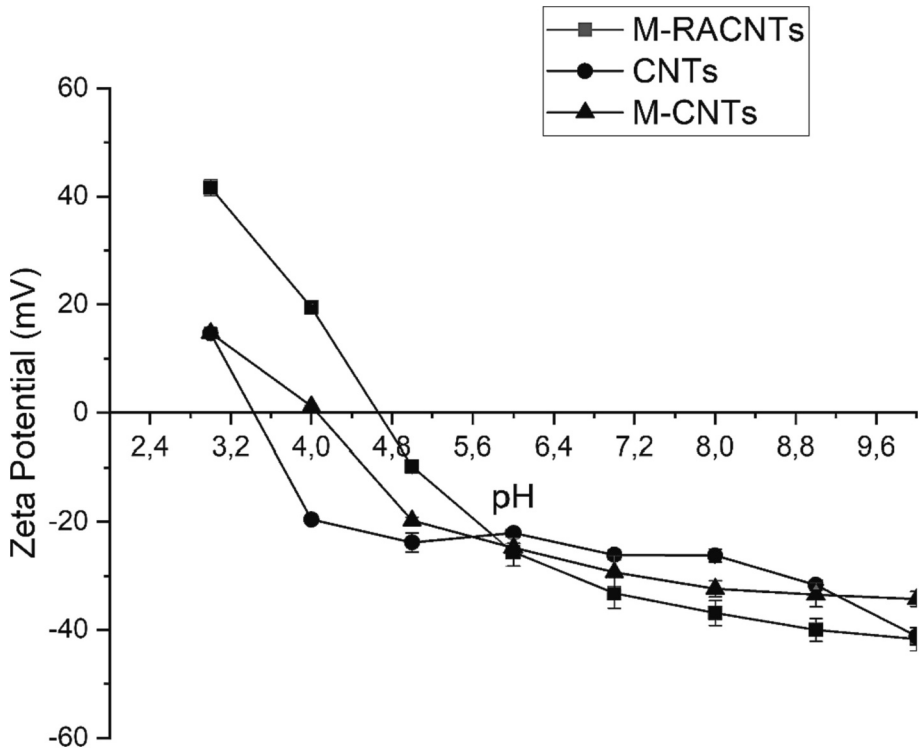

Fig. 3. Zeta potential curves of CNTs, M-CNTs, and M-RACNTs.

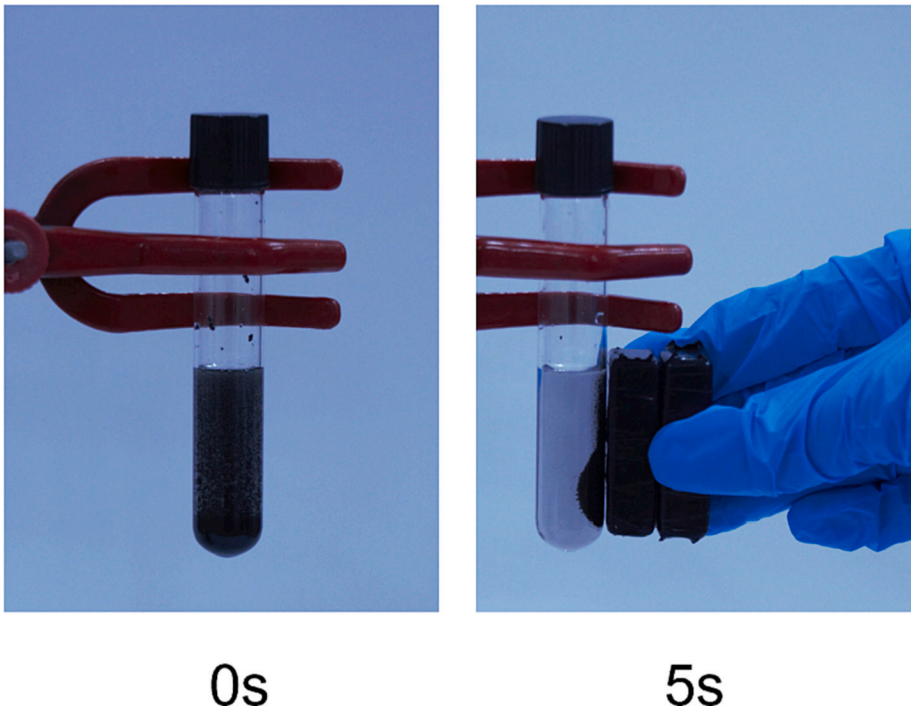

Fig. 4. Use of a neodymium magnet to attract of 100 mg of M-RACNTs particles dispersed in 5 mL of water.

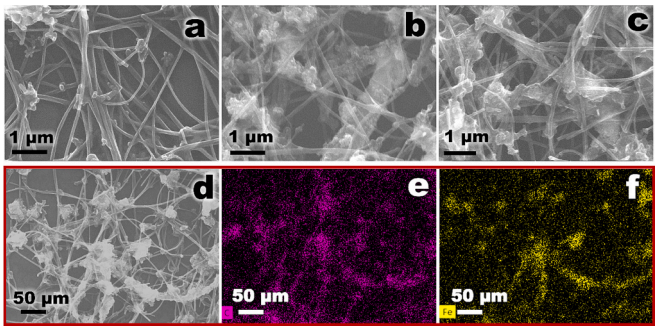

Fig. 5. The SEM image showed the homogeneous distribution of magnetite nanoparticles in carbon nanotubes. a) CNTs; b) M-CNTs, and c–f) M-RACNTs; e) EDS elemental mapping of C Kα of carbon nanotube; f) EDS elemental mapping of Fe Kα of Fe_3O_4 nanoparticles.

by the electron micrographs above.

3.2. Determination of antimicrobial activity

Table 1 shows the antimicrobial activity related to the crude extracts obtained before the optimization of MDSPE. The purpose of these analyses was to evaluate which extracts had antimicrobial activity and the potential to continue in the study. The degree of antimicrobial activity was based on Gómez et al. [1], who established antimicrobial action as strong (<100 μg mL^{-1}), moderate (100–500 μg mL^{-1}), weak (500–1000 μg mL^{-1}), and inactive (≥1000 μg mL^{-1}). These criteria are remarkably similar to those established by Kuete [44] (Table 1).

The chloroform and ethyl acetate extracts showed activity against a Gram-positive pathogen (*Staphylococcus aureus*) (Table 1), while the acetonitrile and hexane extracts did not show activity at the maximum tested concentrations (MIC > 400 μg mL^{-1}). As for the yeast tests, none of the extracts showed significant activity at the maximum concentrations tested (MIC > 400 μg mL^{-1}).

Based on the MIC and MMC values, it was possible to observe that the effectiveness of the chloroform extract was higher than that of the ethyl acetate extract, as lower concentrations were needed to exert bacteriostatic and bactericidal activity. For this reason, chloroform was selected as the elution solvent for the fractional factorial design experiments.

3.3. Analysis of crude extracts by GC–MS and LC-MS/MS

The fermentation broth of *Lasiodiplodia* sp. is a source of organic compounds belonging to different chemical classes [4]. Therefore, according to their chemical structure and the pH of the media, they would interact in different ways with the M-RACNTs' surface and with the elution solvent.

In this way, GC–MS and LC-MS/MS analyses were performed to evaluate the presence of volatile and polar substances in the obtained extracts by MDSPE, and its variation according to the elution solvent used and the fermentation broth pH.

Initially, all the crude extracts were obtained with chloroform, hexane, ethyl acetate, and acetonitrile as an elution solvent, and the pH of the fermentation broth at 3.0, 7.0, and 9.0 (DMSPE procedure described in Section 2.5) was analyzed by CG-MS. It was demonstrated that M-RACNTs presented a good extraction efficiency for volatile compounds at the analyzed elution solvents and pHs, as hydrocarbons, aldehydes, and alcohols, among others (Table 2), were extracted in great amounts.

The substances were identified by comparing the mass spectra obtained with the NIST and Mass Bank databases. According to Table 2, it was possible to observe that when different solvents were used in the elution step (generating the chloroform, hexane, ethyl acetate, and acetonitrile crude extracts), distinct substances were obtained, which was expected due to their different solubilities in the different solvents tested.

The chemical constitution of the different extracts, when only the pH of the fermentation broth was changed (3.0 7.0, or 9.0) and the same elution solvent was used, was the same. However, it was observed that at pH 7.0 higher analytical signals were obtained. For this reason, this pH was chosen to perform the fractional factorial design.

Although all the extracts obtained presented molecules with possible

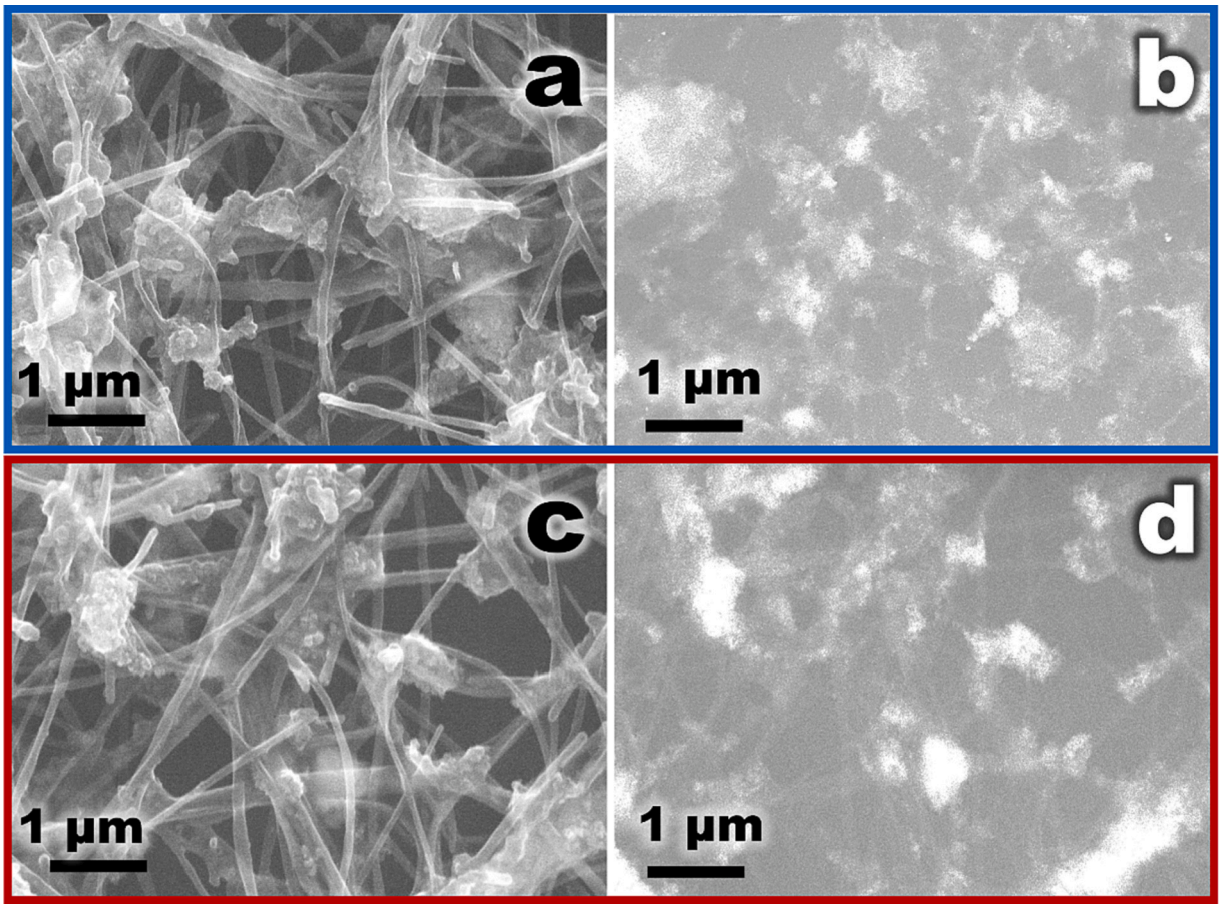

Fig. 6. SEM images provide detailed information on the dispersion of magnetite nanoparticles in the composite. a–b SEM images of M-CNTs nanocomposite; c–d SEM images of M-RACNTs nanocomposite; a–c The secondary electron (SE) SEM images, b–d back-scattered SEM images.

Table 1
Minimal inhibitory concentration (MIC) and minimal microbicidal concentration (MMC) of crude extracts.

Pathogens		Chloroform (μg·mL^{-1})	Ethyl acetate (μg·mL^{-1})	Acetonitrile (μg·mL^{-1})	Hexane (μg·mL^{-1})
Staphylococcus aureus	CIM	100–200	200–400	>400	>400
	CMM	100–200	200–400	N.E.	N.E.
Candida albicans	CIM	>400	>400	>400	>400
	CMM	N.E.	N.E.	N.E.	N.E.
Escherichia coli	CIM	>400	>400	>400	>400
	CMM	N.E.	N.E.	N.E.	N.E.

N.E.: not evaluated.

biological activity, this work evaluated only the antimicrobial activity. Based on the results of the MIC and MMC tests, which showed that the best bacteriostatic and bactericidal activity was for chloroform extracts, and to demonstrate that DMSPE could be optimized to obtain great amounts of a specific compound to the detriment of others, as well as improve the recoveries in future fractionation steps, the decision was made to perform the multivariate optimization for the extraction of hexadecane, a compound with antimicrobial activity already reported in the literature [22,45].

In the chloroform extracts, obtained at pH 7.0, hexadecane peaks (retention time 18.80 min) presented a good chromatographic resolution and great area: important requirements for multivariate optimization. Thus, this substance was selected. Fig. S9 A–B, in the Supplementary Material, show the chromatogram obtained at this condition, and the mass spectra of hexadecane, respectively.

The extracts obtained with different solvents such as chloroform, ethyl acetate, and acetonitrile, were achieved when the pH of the fermentation broth was adjusted at 3.0, 7.0, and 9.0 (the DMSPE procedure described in Section 2.5), were also analyzed by LC-MS. The hexane extract was not evaluated at this step because is a non-polar solvent. Thus, it is capable of extracting the majority of volatile compounds. The spectra obtained by the fragmentation of the selected precursor ions were analyzed in the GNPS platform.

The GNPS online platform is free and based on the storage, analysis, and dissemination of MS/MS spectra. In addition, it allows for community sharing of raw spectra and the grouping and creation of molecular networks (MN) [27]. GNPS has been widely used to accelerate the dereplication of metabolites [46] and to help identify known molecules and new metabolites [47].

Basically, tandem MS data are collected, and the networks are constructed based on similarities of fragment spectra. If a network contains a known substance, identified from a library search, the chemical structure of close members of the network is shown. The MS-based generated network nodes usually correspond to a consensus MS/MS spectrum having an identical precursor mass obtained from various samples. The network nodes are connected by the edges (lines) based on

Table 2
Compounds found in the crude extracts by GC–MS analysis and their corresponding retention time.

Elution solvent	Compound	Retention time (min)
Ethyl acetate	1,5-Pentanediol	5.69
	2-Undecane	10.28
	Nonadecane	11.90
	1-Tretradecene	12.05
	Heptadecane	12.24
	Dodecane	12.37
	Heptadecane	12.49
	Hexadecane	18.80
	Undecane	14.30
	Tridecane	14.70
	Heptadecane	15.01
	Eicosane	19.32
	Tetracosane	20.36
	1,2-Benxenedicarboxylic acid	22.27
	Hexadecanoic acid	24.57
	Tetratricontane	25.29
	Heneicosane	26.40
Acetonitrile	7-Hexadecenal	5.10
	Squalene	22.18
	Hexacontane	23.25
	Octadecane	23.29
	Nonahexacontanoic acid	23.45
	Tetrapentacontane	24.60
	2-Isopropyl-5-methyl-1-heptanol	24.77
	Heneicosane	25.16
	Tetratriacontane	25.43
	Tricontane	25.57
	Tetrapentacontane	25.88
	Dotriacontane	26.05
	Tetracosane	26.67
Chloroform	1-Chloroeicosane	5.09
	Hexadecane	18.80
	Tetrapentacontane	23.31
	Dotriacontane	23.90
	Triacontane	24.64
	Tetrapentacontane	25.07
	Pentatriacontane	25.50
	Eicosane	29.93
	Cholesta-4,6-dien-3-one	30.25
Hexane	Oxirane	5.09
	Cycloheptasiloxane	12.32
	Tetradecanal	13.88
	Squalene	22.26
	Octadecane	22.83
	Triacontanoic acid	22.97
	Cyclononasiloxane	23.02
	Tetratriacontane	23.60
	Tetracosane	23.83
	Eicosane	24.06
	Tricontane	24.16
	Tetrapentacontane	24.40
	Dotricontane	25.06
	Nonacosane	26.09
	18,19-Secoyhimban-19-oic acid	27.68
	1,2-Benzenedicarboxylic acid	28.20

the “cosine score” (similarity core), where the thickness of the edges reflects and measures the positive relatedness of the MS/MS spectra of compounds within a network.

Through the MN analysis, it was possible to observe that chloroform and acetonitrile extracts presented practically the same constituents, such as flavonoids, macrocyclic lactones, jasmonic acid derivatives, and amino acids. Ethyl acetate extracts consisted of flavonoids, macrocyclic lactones, oleic acids, and jasmonic acid derivatives. Table 3 demonstrates the classes and precursors of the identified compounds for each analyzed extract (Table 3).

The pH variation (3.0 or 7.0 or 9.0) did not change the type of substance extracted, however. For volatile compounds analyzed by GC–MS, at pH 7.0, higher analytical signals were obtained when the same elution solvent was used. Thus, this pH was chosen for further tests.

Table 3
Chemical classes of the compounds found in the crude extracts by LC-MS/MS analyses, identified in the GNPS platform, and it is corresponding precursor ions.

Elution solvent	Compound classes	Precursor ions (m/z)
Ethyl acetate	Flavonoids	297, 311, 325 and 325
	Macrocyclic lactones	279 and 391
	Oleic acid derivatives	341 and 359
	jasmonic acid derivatives	185, 199 and 213
Acetonitrile	Flavonoids	297, 311, 325 and 325
	Macrocyclic lactones	279
	jasmonic acid derivatives	185, 199 and 213
	Amino acids	147
Chloroform	Flavonoids	297, 311, 325 and 325
	Macrocyclic lactones	279
	jasmonic acid derivatives	185, 199 and 213
	Amino acids	147

Similar to what was done for volatile compounds, based on the antimicrobial activity test results, to demonstrate the possibility of enhancing the recoveries for a selected compound, the substance with precursor ion $m/z = 213$ $[M + H]^+$ present in the chloroform extract was selected for the multivariate optimization. Likely, this secondary metabolite is a compound derived from jasmonic acid, similar to those identified by Eng et al. [48] from the fermentation broth of *Lasiodiplodia theobromae*. The antimicrobial activity of jasmonic acid and its derivatives was also reported in the literature [23]. The fragment profile of the mass spectrum precursor $m/z = 213$ obtained in this study is shown in Fig. S9 C in the Supplementary Material.

3.4. Fractional factorial design

The optimization of the extraction process was carried out for a volatile compound (hexadecane) analyzed by GC–MS and for a polar compound (jasmonic acid derivative) analyzed by LC-MS/MS using chloroform extracts obtained from the *Lasiodiplodia* sp. fermentation broth at pH 7.00.

In this sense, a 2^{4-1} fractional factorial design with a triplicate of the center point was performed. To determine the proper extraction conditions, the following variables were evaluated: (i) M-RACNTs’ mass (mg); (ii) adsorption time (min); (iii) elution solvent volume (mL); and (iv) desorption time (min).

The real and coded values of the variables to the hexadecane and then to the jasmonic acid derivative are shown in Table S1 in the Supplementary Material, for both compounds. Below, the data for hexadecane will be described first; this will be followed by the data for the jasmonic acid derivative.

Before evaluating the best conditions for the extraction of the two compounds, it is necessary to evaluate the quality of the linear model obtained from the 2^{4-1} fractional factorial design. To check the quality of the linear model, an analysis of variance (ANOVA) was performed. After data processing, the evaluation of the best conditions for the extraction was performed by an analysis of the Pareto graphic, evaluating the significance of the variables and their interactions, at a confidence level of 95 %. The results are shown in Table S2 in the Supplementary Material. The good agreement between the predicted and experimental values can be seen in the Supplementary Material, Fig. S10.

Based on the results presented in the Pareto graphic (Fig. 7), one can see that the mass of M-RACNTs (estimated positive effect), elution solvent volume (estimated negative effect), and interactions between the mass of M-RACNTs versus the desorption time and the mass of M-RACNTs versus the elution solvent volume (both estimated negative effects) were statistically significant ($p < 0.05$). The main effects of desorption and adsorption times were not relevant in the hexadecane extraction in the experimental domain.

This result means that large amounts of mass and lower amounts of elution solvent increase the analyte recovery. The use of a low elution

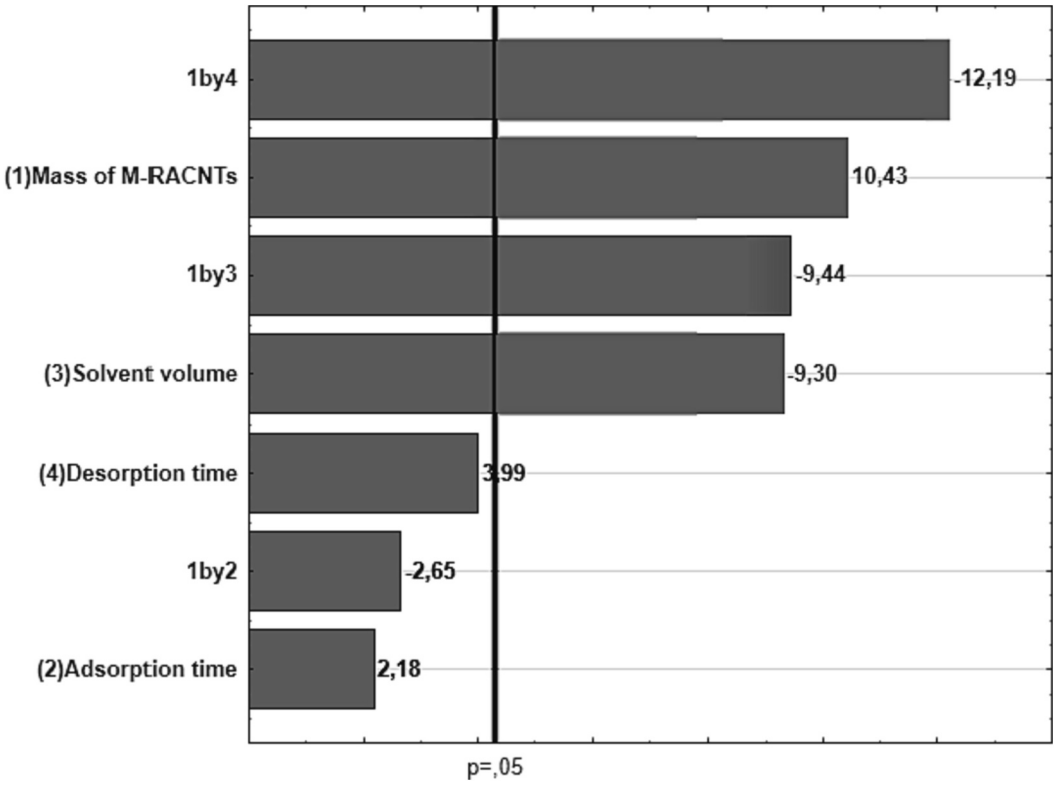

Fig. 7. Pareto Chart for the estimated effect of the factors and their interactions for hexadecane.

solvent volume contributes to an increase in the preconcentration factor. According to the graph, it is also possible to conclude that a long desorption time favors the desorption of other substances and improves the matrix effect, decreasing the analytical signal.

For the jasmonic acid derivative, the quality of the linear model obtained from a 2^{4-1} fractional factorial design was also evaluated by ANOVA. The data are shown in Table S3 in the Supplementary Material. The good agreement between the predicted and experimental values can

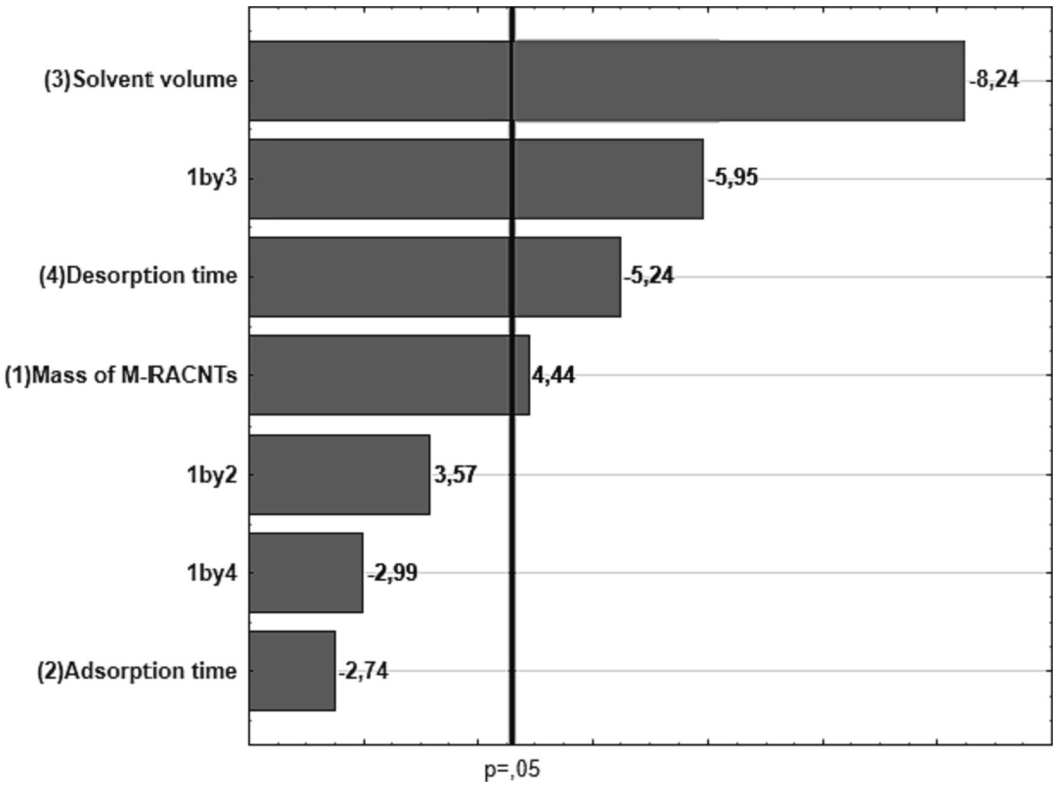

Fig. 8. Pareto Chart for the estimated effect of the factors and their interactions for the jasmonic acid derivative.

be seen in the Supplementary Material, Fig. S11.

According to the results presented in the Pareto graphic (Fig. 8), the elution solvent volume, desorption time (estimated negative effect), the mass of M-RACNTs (estimated positive effect), and interaction between M-RACNTs versus elution solvent volume (estimated negative effects) were statistically significant ($p < 0.05$). The main effect of adsorption time was not relevant.

From the results, it can be observed that when a large amount of M-RACNTs mass, a low volume of elution solvent, and a short desorption time are used, a greater analytical response is obtained. Similar to what happens to hexadecane, the use of more material and a small quantity of solvent improves the pre-concentration factor, while long periods of desorption favor the desorption of other substances and cause ionic suppression, decreasing analyte ionization and, consequently, generating a low analytical response.

Therefore, the optimized conditions for the DMSPE procedure for hexadecane and the jasmonic acid derivative were 150 mg of M-RACNTs, 3.0 mL of chloroform, 30 min of adsorption time, and 10 min of desorption time. As can be observed, under the optimized conditions, it is possible to obtain an extract richer in two substances with bacteriostatic and bactericidal activities, which is important to improve recoveries in future fractionation steps.

3.5. SDS-PAGE analysis

To evaluate the capacity to exclude macromolecules, such as proteins, by M-RACNTs, the fermentation broth left over from the extraction process was evaluated by SDS-PAGE analysis. Fig. 9 shows the gel obtained. It is possible to observe that the protein constitution of the fermentation broth of *Lasiodiplodia* sp., probably, is a major lysozyme (14.4 kD standard), and that the macromolecule exclusion was more efficient at a pH of 7.0, as a strong spot corresponding to this enzyme can be seen at this pH.

The exclusion of proteins by RAM is based on chemistry and physics mechanisms, in which the hydrophilic barrier, in this case, provided by the BSA layer, prevents the adsorption of macromolecules and allows small molecules to cross the hydrophilic barrier to be retained by the adsorbent [15].

The results obtained by SDS-PAGE analysis corroborate the fact that higher analytical signals, for both volatile and non-volatile compounds, were obtained when the pH of the fermentation broth was adjusted to 7.0 and that, in fact, the presence of proteins negatively affects the efficiency of extraction of low molecular weight compounds.

4. Conclusions

In this study, a magnetic RAM (M-RACNTs) was obtained by the incorporation of magnetic nanoparticles and by modifying the surface of commercial multi-walled carbon nanotubes. Comprehensive physical characterization involving FT-IR, thermogravimetric, zeta potential, and scanning electron microscopy confirmed the successful synthesis of the sorbent M-RACNTs exhibited substantial potential as a sorbent in MDSPE, effectively extracting organic compounds from the fermentation broth of the endophyte *Lasiodiplodia* sp. Notably, this proposed method facilitated the extraction of biologically active substances, with biological activity potential, like bacteriostatic and bactericidal activities. Utilizing multivariate optimization, it was possible to identify statistically significant factors to enhance the extraction of hexadecane and a jasmonic acid derivative. This optimization enabled the extraction of crude extracts with high concentrations of these compounds, priming them for subsequent fractionation and isolation processes. Finally, the MDSPE method based on M-RACNTs emerges as an alternative to replace conventional LLE to potentially reduce the requirement for large sample sizes and organic solvent volumes.

CRediT authorship contribution statement

Cristiane dos R. Feliciano: Investigation, Writing – original draft. **Heloisa Sales de Souza:** Investigation. **Vinicius Câmara Costa:** Formal analysis, Writing – review & editing. **Omar Cabezas Gómez:** Investigation. **Jaine Honorata Hortolan Luiz:** Resources, Writing – review & editing. **Luiz Fernando Gorup:** Investigation, Resources, Writing – review & editing. **Mariane Gonçalves Santos:** Conceptualization, Funding acquisition, Project administration, Resources, Supervision, Writing

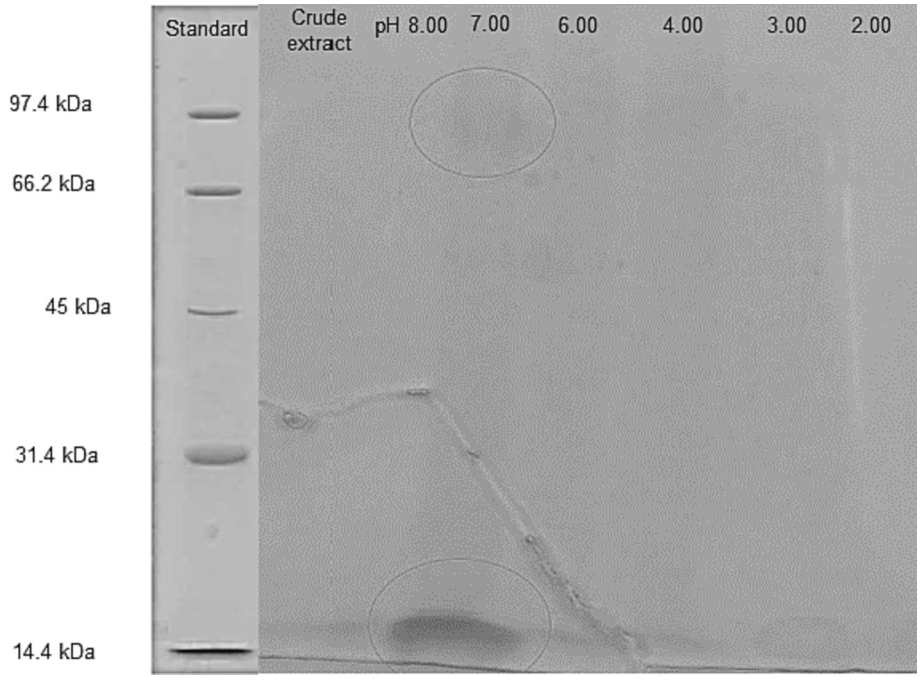

Fig. 9. (a) SDS-PAGE of the fermentation broth left over from the extraction process: (1) markers (low range 14.4 to 97.4 kDa); (2) pH = 8.0; (3) pH = 7.0; (4) pH = 6.0; (5) pH = 5.0; (6) pH = 4.0; (7) pH = 3.0; (8) broth without extraction and (9) fermentation broth left over from the extraction process without pH adjustment.

– review & editing.

Declaration of competing interest

The authors declare the following financial interests/personal relationships which may be considered as potential competing interests: Cristiane Dos Reis Feliciano reports financial support was provided by Coordination of Higher Education Personnel Improvement. Heloisa Sales de Souza reports financial support was provided by Coordination of Higher Education Personnel Improvement. Mariane Goncalves Santos reports financial support was provided by Minas Gerais State Foundation of Support to the Research. Luiz Fernando Gorup reports financial support was provided by State of Sao Paulo Research Foundation.

Data availability

No data was used for the research described in the article.

Acknowledgements

The authors acknowledge the Universidade Federal de Alfenas (UNIFAL), Fundação de Amparo à Pesquisa do Estado de Minas Gerais (FAPEMIG) (grant number APQ-00782-18), Fundação de Amparo à Pesquisa do Estado de São Paulo (FAPESP) (grant numbers 2012/07067-0,2013/23572-0, 2016/019405, and 2013/07296), Centro de Pesquisa, Inovação e Difusão (CEPID) (grant number 2013/07296-2); Instituto Nacional de Ciência e Tecnologia dos Materiais em Nanotecnologia (INCTMN) (grant number 2008/57872-1), and Conselho Nacional de Desenvolvimento Científico e Tecnológico (CNPq) (grant numbers 573636/2008-7, 435975/2018-8, 421648/2018-0) for financial support. Special thanks to the Coordenação de Aperfeiçoamento de Pessoal de Nível Superior (CAPES - Brazil) - Finance Code 001 for technical support and the concession of a scholarship.

Appendix A. Supplementary data

Supplementary data to this article can be found online at https://doi.org/10.1016/j.diamond.2023.110763.

References

[1] O.C. Gómez, D.M.B. Moreira, I.L.C. Hernández, R.M.L. Lemes, J.H.H. Luiz, Antimicrobial activity improvement after fractionating organic extracts from Lasiodiplodia Sp. fermentation/Melhoria Da Atividade Antimicrobiana Após Fracionamento De Extratos Orgânicos De Lasiodiplodia Sp. Fermentação, Brazil. J. Dev. 7 (2021) 3795–3816, https://doi.org/10.34117/bjdv7n1-257.

[2] M.M. Salvatore, A. Alves, A. Andolfi, Secondary metabolites of lasiodiplodia theobromae: distribution, chemical diversity, bioactivity, and implications of their occurrence, Toxins (Basel) 12 (2020), https://doi.org/10.3390/toxins12070457.

[3] S.C.N. Queiroz, C.H. Collins, Métodos de Extração e/ou Concentração de Compostos Encontrados em Fluidos Biológicos para Posterior Determinação Cromatográfica 24, 2001, pp. 68–76.

[4] F.C. Oliveira, F.G. Barbosa, J. Mafezoli, M.D.C.F. De Oliveira, F.J.T. Gonçalves, F.C. O. Freire, Perfil dos componentes voláteis produzidos pelo fungo fitopatógeno albonectria rigidiuscula em diferentes condições de cultivo, Quim Nova 40 (2017) 890–894, https://doi.org/10.21577/0100-4042.20170064.

[5] S.J. Yue, M. Bilal, C. Song, S.Q. Guo, S. Li, P. Huang, H.B. Hu, W. Wang, X. H. Zhang, Development of an efficient method for separation and purification of trans-2,3-dihydro-3-hydroxyanthranilic acid from Pseudomonas chlororaphis GP72 fermentation broth, Sep. Purif. Technol. 202 (2018) 144–148, https://doi.org/10.1016/j.seppur.2018.03.036.

[6] H. Bagheri, R. Daliri, A. Roostaie, A novel magnetic poly(aniline-naphthylamine)-based nanocomposite for micro solid phase extraction of rhodamine B, Anal. Chim. Acta 794 (2013) 38–46, https://doi.org/10.1016/j.aca.2013.07.066.

[7] A.A. Asgharinezhad, H. Ebrahimzadeh, F. Mirbabaei, N. Mollazadeh, N. Shekari, Dispersive micro-solid-phase extraction of benzodiazepines from biological fluids based on polyaniline/magnetic nanoparticles composite, Anal. Chim. Acta 844 (2014) 80–89, https://doi.org/10.1016/j.aca.2014.06.007.

[8] A.R. Bagheri, M. Arabi, M. Ghaedi, A. Ostovan, X. Wang, J. Li, L. Chen, Dummy molecularly imprinted polymers based on a green synthesis strategy for magnetic solid-phase extraction of acrylamide in food samples, Talanta 195 (2019) 390–400, https://doi.org/10.1016/j.talanta.2018.11.065.

[9] M. Arabi, M. Ghaedi, A. Ostovan, Development of a lower toxic approach based on green synthesis of water-compatible molecularly imprinted nanoparticles for the extraction of hydrochlorothiazide from human urine, ACS Sustain. Chem. Eng. 5 (2017) 3775–3785, https://doi.org/10.1021/acssuschemeng.6b02615.

[10] K. Molaei, H. Bagheri, A.A. Asgharinezhad, H. Ebrahimzadeh, M. Shamsipur, SiO2-coated magnetic graphene oxide modified with polypyrrole–polythiophene: a novel and efficient nanocomposite for solid phase extraction of trace amounts of heavy metals, Talanta 167 (2017) 607–616, https://doi.org/10.1016/j.talanta.2017.02.066.

[11] Y. Yamini, M. Safari, A. Morsali, V. Safarifard, Magnetic frame work composite as an efficient sorbent for magnetic solid-phase extraction of plasticizer compounds, J. Chromatogr. A 1570 (2018) 38–46, https://doi.org/10.1016/j.chroma.2018.07.069.

[12] N. Jalilian, H. Ebrahimzadeh, A.A. Asgharinezhad, A nanosized magnetic metal-organic framework of type MIL-53(Fe) as an efficient sorbent for coextraction of phenols and anilines prior to their quantitation by HPLC, Microchim. Acta 186 (2019), https://doi.org/10.1007/s00604-019-3698-9.

[13] N. Jalilian, H. Ebrahimzadeh, A.A. Asgharinezhad, Preparation of magnetite/multiwalled carbon nanotubes/metal-organic framework composite for dispersive magnetic micro solid phase extraction of parabens and phthalate esters from water samples and various types of cream for their determination with liquid, J. Chromatogr. A 1608 (2019) 460426, https://doi.org/10.1016/j.chroma.2019.460426.

[14] A. Campos do Lago, M.H. da Silva Cavalcanti, M.A. Rosa, A.T. Silveira, C.R. Teixeira Tarley, E.C. Figueiredo, Magnetic restricted-access carbon nanotubes for dispersive solid phase extraction of organophosphates pesticides from bovine milk samples, Anal. Chim. Acta 1102 (2020) 11–23, https://doi.org/10.1016/j.aca.2019.12.039.

[15] H.D. de Faria, L.C. de C. Abrão, M.G. Santos, A.F. Barbosa, E.C. Figueiredo, New advances in restricted access materials for sample preparation: a review, Anal. Chim. Acta 959 (2017) 43–65, https://doi.org/10.1016/j.aca.2016.12.047.

[16] Y.Z. Baghdady, K.A. Schug, Evaluation of efficiency and trapping capacity of restricted access media trap columns for the online trapping of small molecules, J. Sep. Sci. 39 (2016) 4183–4191, https://doi.org/10.1002/jssc.201600777.

[17] M.G. Santos, I.M.C. Tavares, V.B. Boralli, E.C. Figueiredo, Direct doping analysis of beta-blocker drugs from urinary samples by on-line molecularly imprinted solid-phase extraction coupled to liquid chromatography/mass spectrometry, Analyst 140 (2015) 2696–2703, https://doi.org/10.1039/c4an02066a.

[18] J.C. Cruz, H.D. de Faria, E.C. Figueiredo, M.E.C. Queiroz, Restricted access carbon nanotube for microextraction by packed sorbent to determine antipsychotics in plasma samples by high-performance liquid chromatography-tandem mass spectrometry, Anal. Bioanal. Chem. 412 (2020) 2465–2475, https://doi.org/10.1007/s00216-020-02464-4.

[19] J. Feng, X. He, X. Liu, X. Sun, Y. Li, Preparation of magnetic graphene/mesoporous silica composites with phenyl-functionalized pore-walls as the restricted access matrix solid phase extraction adsorbent for the rapid extraction of parabens from water-based skin toners, J. Chromatogr. A 1465 (2016) 20–29, https://doi.org/10.1016/j.chroma.2016.08.052.

[20] S. Qu, F. Huang, G. Chen, S. Yu, J. Kong, Magnetic assembled electrochemical platform using Fe2O3 filled carbon nanotubes and enzyme, Electrochem. Commun. 9 (2007) 2812–2816, https://doi.org/10.1016/j.elecom.2007.09.021.

[21] A.F. Barbosa, V.M.P. Barbosa, J. Bettini, P.O. Luccas, E.C. Figueiredo, Restricted access carbon nanotubes for direct extraction of cadmium from human serum samples followed by atomic absorption spectrometry analysis, Talanta 131 (2015) 213–220, https://doi.org/10.1016/j.talanta.2014.07.051.

[22] O.E. Falade, V.O. Oyetayo, S.I. Awala, Evaluation of the mycochemical composition and antimicrobial potency of wild macrofungus, *Rigidoporus microporus* (Sw), J. Phytopharm. 6 (2017) 115–125.

[23] U. Złotek, M. Michalak-majewska, R.-T. Kamila, applied sciences and α-Amylase Inhibitory Activity, as well as Antimicrobial Activities, of Essential Oil from Lettuce Leaf Basil (*Ocimum basilicum* L.) Elicited with Jasmonic Acid, (n.d.) 1–12.

[24] T. Pluskal, S. Castillo, A. Villar-Briones, M. Orešič, MZmine 2: modular framework for processing, visualizing, and analyzing mass spectrometry-based molecular profile data, BMC Bioinformatics. 11 (2010), https://doi.org/10.1186/1471-2105-11-395.

[25] M. Katajamaa, J. Miettinen, M. Orešič, MZmine: toolbox for processing and visualization of mass spectrometry based molecular profile data, Bioinformatics 22 (2006) 634–636, https://doi.org/10.1093/bioinformatics/btk039.

[26] L.F. Nothias, D. Petras, R. Schmid, K. Dührkop, J. Rainer, A. Sarvepalli, I. Protsyuk, M. Ernst, H. Tsugawa, M. Fleischauer, F. Aicheler, A.A. Aksenov, O. Alka, P. M. Allard, A. Barsch, X. Cachet, A.M. Caraballo-Rodriguez, R.R. Da Silva, T. Dang, N. Garg, J.M. Gauglitz, A. Gurevich, G. Isaac, A.K. Jarmusch, Z. Kameník, K. Bin Kang, N. Kessler, I. Koester, A. Korf, A. Le Gouellec, M. Ludwig, C. Martin H, L. I. McCall, J. McSayles, S.W. Meyer, H. Mohimani, M. Morsy, O. Moyne, S. Neumann, H. Neuweger, N.H. Nguyen, M. Nothias-Esposito, J. Paolini, V. V. Phelan, T. Pluskal, R.A. Quinn, S. Rogers, B. Shrestha, A. Tripathi, J.J.J. van der Hooft, F. Vargas, K.C. Weldon, M. Witting, H. Yang, Z. Zhang, F. Zubeil, O. Kohlbacher, S. Böcker, T. Alexandrov, N. Bandeira, M. Wang, P.C. Dorrestein, Feature-based molecular networking in the GNPS analysis environment, Nat. Methods 17 (2020) 905–908, https://doi.org/10.1038/s41592-020-0933-6.

[27] M. Wang, J.J. Carver, V.V. Phelan, L.M. Sanchez, N. Garg, Y. Peng, D.D. Nguyen, J. Watrous, C.A. Kapono, T. Luzzatto-Knaan, C. Porto, A. Bouslimani, A.V. Melnik, M.J. Meehan, W.T. Liu, M. Crüsemann, P.D. Boudreau, E. Esquenazi, M. Sandoval-Calderón, R.D. Kersten, L.A. Pace, R.A. Quinn, K.R. Duncan, C.C. Hsu, D.J. Floros, R.G. Gavilan, K. Kleigrewe, T. Northen, R.J. Dutton, D. Parrot, E.E. Carlson, B. Aigle, C.F. Michelsen, L. Jelsbak, C. Sohlenkamp, P. Pevzner, A. Edlund,

J. McLean, J. Piel, B.T. Murphy, L. Gerwick, C.C. Liaw, Y.L. Yang, H.U. Humpf, M. Maansson, R.A. Keyzers, A.C. Sims, A.R. Johnson, A.M. Sidebottom, B.E. Sedio, A. Klitgaard, C.B. Larson, C.A.P. Boya, D. Torres-Mendoza, D.J. Gonzalez, D. B. Silva, L.M. Marques, D.P. Demarque, E. Pociute, E.C. O'Neill, E. Briand, E.J. N. Helfrich, E.A. Granatosky, E. Glukhov, F. Ryffel, H. Houson, H. Mohimani, J. J. Kharbush, Y. Zeng, J.A. Vorholt, K.L. Kurita, P. Charusanti, K.L. McPhail, K. F. Nielsen, L. Vuong, M. Elfeki, M.F. Traxler, N. Engene, N. Koyama, O.B. Vining, R. Baric, R.R. Silva, S.J. Mascuch, S. Tomasi, S. Jenkins, V. Macherla, T. Hoffman, V. Agarwal, P.G. Williams, J. Dai, R. Neupane, J. Gurr, A.M.C. Rodríguez, A. Lamsa, C. Zhang, K. Dorrestein, B.M. Duggan, J. Almaliti, P.M. Allard, P. Phapale, L.F. Nothias, T. Alexandrov, M. Litaudon, J.L. Wolfender, J.E. Kyle, T. O. Metz, T. Peryea, D.T. Nguyen, D. VanLeer, P. Shinn, A. Jadhav, R. Müller, K. M. Waters, W. Shi, X. Liu, L. Zhang, R. Knight, P.R. Jensen, B. Palsson, K. Pogliano, R.G. Linington, M. Gutiérrez, N.P. Lopes, W.H. Gerwick, B.S. Moore, P. C. Dorrestein, N. Bandeira, Sharing and community curation of mass spectrometry data with global natural products social molecular networking, Nat. Biotechnol. 34 (2016) 828–837, https://doi.org/10.1038/nbt.3597.

[28] U.K. Laemmli, Cleavage of structural proteins during the assembly of the head of bacteriophage T4, Nature 227 (1970) 680–685.

[29] D.I.B.R.M. Silverstein, F.X. Webster, D.J. Kiemle, Spectrometric Identification of Organic Compounds, 8° ed, John Wiley & Sons, 2019.

[30] M.A. Rosa, H.D. De Faria, D.T. Carvalho, E.C. Figueiredo, Biological sample preparation by using restricted-access nanoparticles prepared from bovine serum albumin: application to liquid chromatographic determination of β-blockers, Microchim. Acta. 186 (2019), https://doi.org/10.1007/s00604-019-3774-1.

[31] Y. Hu, C. Guo, in: D.M. Naraghi (Ed.), Carbon Nanotubes and Carbon Nanotubes/Metal Oxide Heterostructures: Synthesis, Characterization and Electrochemical Property, IntechOpen, Rijeka, 2011, https://doi.org/10.5772/16463 p. Ch. 1.

[32] Y. Yang, T. Li, Y. Qin, L. Zhang, Y. Chen, Construct of carbon nanotube-supported Fe2O3 hybrid Nanozyme by atomic layer deposition for highly efficient dopamine sensing, Front. Chem. 8 (2020).

[33] J. Yao, Y. Li, J. Yan, J. Jiang, S. Xiao, ZnFe2O4 nanoparticles imbedding in carbon prepared from leaching liquor of jarosite residue as anode material for lithium-ion batteries, Ionics (Kiel) 26 (2020) 4373–4380, https://doi.org/10.1007/s11581-020-03583-9.

[34] M. Valášková, J. Tokarský, J. Pavlovský, T. Prostějovský, K. Kočí, α-Fe2O3 nanoparticles/vermiculite clay material: structural, optical and photocatalytic properties, Materials (Basel) 12 (2019), https://doi.org/10.3390/ma12111880.

[35] W. Li, X. Li, J. Liu, M. Zeng, X. Feng, X. Jia, Z.-Z. Yu, Coating of wood with Fe2O3-decorated carbon nanotubes by one-step combustion for efficient solar steam generation, ACS Appl. Mater. Interfaces 13 (2021) 22845–22854, https://doi.org/10.1021/acsami.1c03388.

[36] M. Najafi, S. Bellani, V. Galli, M.I. Zappia, A. Bagheri, M. Safarpour, H. Beydaghi, M. Eredia, L. Pasquale, R. Carzino, S. Lauciello, J.-K. Panda, R. Brescia, L. Gabatel, V. Pellegrini, F. Bonaccorso, Carbon-α-Fe2O3 composite active material for high-capacity electrodes with high mass loading and flat current collector for quasi-symmetric supercapacitors, Electrochem 3 (2022) 463–478, https://doi.org/10.3390/electrochem3030032.

[37] P. Cui, A. Wang, Synthesis of CNTs/CuO and its catalytic performance on the thermal decomposition of ammonium perchlorate, J. Saudi Chem. Soc. 20 (2016) 343–348, https://doi.org/10.1016/j.jscs.2014.09.010.

[38] R. Siddheswaran, D. Manikandan, R.E. Avila, C.E. Jeyanthi, R.V. Mangalaraja, Formation of carbon nanotube forest over spin-coated Fe2O3 reduced thin-film by chemical vapor deposition, fullerenes, Nanotub. Carbon Nanostruct. 23 (2015) 392–398, https://doi.org/10.1080/1536383X.2013.866945.

[39] H.A. Asmaly, B. Abussaud, T.A. Ihsanullah, V.K. Saleh, M.A. Atieh Gupta, Ferric oxide nanoparticles decorated carbon nanotubes and carbon nanofibers: from synthesis to enhanced removal of phenol, J. Saudi Chem. Soc. 19 (2015) 511–520, https://doi.org/10.1016/j.jscs.2015.06.002.

[40] H. Nakajima, T. Morimoto, Y. Zhou, K. Kobashi, S. Ata, T. Yamada, T. Okazaki, Nonuniform functional group distribution of carbon nanotubes studied by energy dispersive X-ray spectrometry imaging in SEM, Nanoscale 11 (2019) 21487–21492, https://doi.org/10.1039/C9NR07619K.

[41] J.A. Ramos-Guivar, F.J. Litterst, E.C. Passamani, AC susceptibility studies under DC fields in superspinglass nanomaghemite-multiwall carbon nanotube hybrid, Magnetochemistry 7 (2021), https://doi.org/10.3390/magnetochemistry7040052.

[42] A.-G. Niculescu, C. Chircov, A.M. Grumezescu, Magnetite nanoparticles: synthesis methods – a comparative review, Methods 199 (2022) 16–27, https://doi.org/10.1016/j.ymeth.2021.04.018.

[43] H. Fatima, D.-W. Lee, H.J. Yun, K.-S. Kim, Shape-controlled synthesis of magnetic Fe(3)O(4) nanoparticles with different iron precursors and capping agents, RSC Adv. 8 (2018) 22917–22923, https://doi.org/10.1039/c8ra02909a.

[44] V. Kuete, Potential of Cameroonian plants and derived products against microbial infections: a review, Planta Med. 76 (2010) 1479–1491, https://doi.org/10.1055/s-0030-1250027.

[45] S. Yogeswari, S. Ramalakshmi, R. Neelavathy, J. Muthumary, Identification and comparative studies of different volatile fractions from Monochaetia kansensis by GCMS, Glob. J. Pharmacol. 6 (2012) 65–71.

[46] G.G. De Oliveira, F. Carnevale Neto, D.P. Demarque, J.A. De Sousa Pereira-Junior, R.C. Sampaio Peixoto Filho, S.J. De Melo, J.R.G. Da Silva Almeida, J.L.C. Lopes, N. P. Lopes, Dereplication of flavonoid glycoconjugates from Adenocalymma imperatoris-maximilianii by untargeted tandem mass spectrometry-based molecular networking, Planta Med. 83 (2017) 636–646, https://doi.org/10.1055/s-0042-118712.

[47] C. Taboada, A.E. Brunetti, F.N. Pedron, F.C. Neto, D.A. Estrin, S.E. Bari, L. B. Chemese, N.P. Lopes, M.G. Lagorio, J. Faivovich, Naturally occurring fluorescence in frogs, Proc. Natl. Acad. Sci. U. S. A. 114 (2017) 3672–3677, https://doi.org/10.1073/pnas.1701053114.

[48] F. Eng, S. Haroth, K. Feussner, D. Meldau, D. Rekhter, T. Ischebeck, F. Brodhun, I. Feussner, Optimized jasmonic acid production by Lasiodiplodia theobromae reveals formation of valuable plant secondary metabolites, PloS One 11 (2016) 1–18, https://doi.org/10.1371/journal.pone.0167627.